DOI: 10.1021/ic1007439

Inorganic Chemistry
Article

Hg^{2+} Detection by New Anthracene Pendant-Arm Derivatives of Mixed N/S- and N/S/O-Donor Macrocycles: Fluorescence, Matrix-Assisted Laser Desorption/Ionization Time-of-Flight Mass Spectrometry and Density Functional Theory Studies

Marta Mameli,[†] Vito Lippolis,*[,†] Claudia Caltagirone,[†] José Luis Capelo,[‡,§] Olalla Nieto Faza,*[,⊥] and Carlos Lodeiro*[,‡,§]

[†]*Dipartimento di Chimica Inorganica ed Analitica, Università degli Studi di Cagliari, S.S. 554 Bivio per Sestu, 09042 Monserrato, Italy,* [‡]*Grupo BIOSCOPE, Departamento de Química-Física, Facultad de Ciencias de Ourense, Universidad de Vigo, E-32004 Ourense, Spain,* [§]*REQUIMTE-CQFB, Departamento de Química, FCT, Universidade Nova de Lisboa, Monte de Caparica 2829-516, Portugal, and* [⊥]*Departamento de Química Orgánica, Facultade de Ciencias de Ourense, Universidade de Vigo, E-32004 Ourense, Spain*

Received April 18, 2010

The optical response of four new anthracenylmethyl pendant-arm derivatives (**L1**−**L4**) of the macrocyclic ligands [12]aneNS$_3$, [12]aneNS$_2$O, [15]aneNS$_2$O$_2$, and [12]aneN$_2$SO toward the metal ions Zn^{2+}, Cd^{2+}, Pb^{2+}, Cu^{2+}, Hg^{2+}, Ag^{+}, Fe^{2+}, Co^{2+}, Ni^{2+}, Mn^{2+}, Ca^{2+}, Na^{+}, Mg^{2+}, and K^{+} was investigated in 1:1 (v/v) MeCN/H$_2$O solutions. A strong chelation enhancement of quenching effect was observed on the fluorescent emission intensity of **L2** as a consequence of the *host*−*guest* interaction with Hg^{2+} and the formation of a 1:2 metal-to-ligand complex. Density functional theory calculations confirmed the formation of a sandwich-type complex between **L2** and Hg^{2+} as a favorable process. A matrix-assisted laser desorption/ionization (MALDI) time-of-flight mass spectrometry study using the four ligands as active MALDI probes was also performed. **L1**−**L4** have also been explored as fluorescence chemosensors in microsamples using NANODROP technology.

Introduction

Mercury(II) is the most contaminant of the hard metal ions, with complex and uncommon chemical and physical properties. It is well-known that heavy-metal ions such as mercury(II), cadmium(II), or lead(II) are dangerous to human beings because they tend to bioaccumulate in the organism, increasing their concentrations over time at the cellular level, thus causing dangerous conditions of intoxication and adverse effects upon human health.[1] Chemical processes such as methylation of mercury(II) can increase the concentration in tissues and amplify the bioavailability of this metal in living organisms, especially in shellfish and fish.[1,2] These organic mercury(II) derivatives such as monomethylmercury(II) and dimethylmercury(II) are extremely toxic[3] and cause neurotoxicological disorders.[4] All of this has prompted the development of detection and monitoring analytical technologies aiming at measuring this metal and its organic derivatives in samples of biological, environmental, agricultural, and food provenance.[5]

Up until now, many sensitive and accurate analytical techniques have been used for mercury detection, such as nuclear magnetic resonance spectroscopy,[6] atomic absorption and mass spectrometry,[7] or mercury extraction from

*To whom correspondence should be addressed. E-mail: lippolis@unica.it (V.L.), faza@uvigo.es (O.N.F.), clodeiro@uvigo.es (C.L.). Tel.: +39 070 675 4467 (V.L.), +34 986 813721 (O.N.F.), 34 988 368894 (C.L.). Fax: +39 070 675 4456 (V.L.), +34 988 387001 (O.N.F.), +34 988 387001 (C.L.).

(1) (a) Vernet, P. *Heavy Metals in the Environment*; Elsevier: New York, 1991. (b) Sigel, A.; Sigel, H.; Sigel, R. K. O. Metal Ions in Life Sciences. *Neurodegenerative Diseases and Metal Ions*; John Wiley & Sons: Chichester, U.K., 2006; Vol. *1*. (c) Nordberg, G. F.; Fowler, B. A.; Nordberg, M.; Friberg, L. *Handbook on the Toxicology of Metals*, 3rd ed.; Elsevier Inc.: New York, 2007.

(2) (a) Southworth, G. R.; Turner, R. R.; Peterson, M. J.; Bogle, M. A.; Ryon, M. G. *Environ. Monit. Assess.* **2000**, *63*, 481. (b) Hrabik, T. R.; Watras, C. J. *Sci. Total Environ.* **2002**, *297*, 229. (c) Sorensen, J. A.; Kallemyn, L. W.; Sydor, M. *Environ. Sci. Technol.* **2005**, *39*, 9237. (d) Leermakers, M.; Baeyens, W.; Quevauviller, P.; Horvat, M. *Trends Anal. Chem.* **2005**, *24*, 383.

(3) Havarinasab, S.; Hultman, P. *Autoimmun. Rev.* **2005**, *4*, 270.

(4) Day, J. J.; Reed, M. N.; Newland, M. C. *Neurotoxicol. Teratol.* **2005**, *27*, 629.

(5) (a) Liu, Y.; Zai, Y.; Chang, X.; Guo, Y.; Meng, S.; Feng, F. *Anal. Chim. Acta* **2006**, *575*, 159. (b) Capelo, J. L.; Lavilla, I.; Bendicho, C. *Anal. Chem.* **2000**, *72*, 4979. (c) Capelo, J. L.; Maduro, C.; Mota, A. M. *J. Anal. Atom. Spectrom.* **2004**, *19*, 414.

(6) Helm, M. L.; Helton, G. P.; Van Derveer, D. G.; Grant, G. J. *Inorg. Chem.* **2005**, *44*, 5696 and references cited therein.

(7) (a) Capelo, J. L.; Maduro, C.; Mota, A. M. *Ultrason. Sonochem.* **2006**, *13*, 98. (b) Ubillus, F.; Alegria, A.; Barbera, R.; Farre, R.; Lagarda, M. J. *Food Chem.* **2000**, *71*, 529.

Published on Web 08/17/2010

aqueous solutions or organic media,[8] but most of these detection techniques are sample-destructive methods. Of the nondestructive-sample analytical methodologies, the most important are those based on optical devices such as chromogenic sensors or fluorescent chemosensors,[9−11] which offer many advantages in terms of selectivity, sensitivity, response time, and cost.[12−22]

The most common synthetic approach to the synthesis of fluorescent molecular sensors is to link covalently, through an appropriate spacer, a fluorogenic fragment (signaling unit) to a guest-binding site (receptor unit). The interaction of the target species with the receptor unit elicits an optical signal expressed as an enhancement or quenching of the fluorophore emission.[12−22]

The choice of the read-out or signaling unit can be critical to both the performance and the selectivity of the sensor, especially if direct interaction between the fluorophore and the target species is possible.

However, the chemosensor selectivity would be determined solely or mainly by the nature of the receptor unit, whereas the transduction mechanism that is triggered by the host−guest interaction and the sensitivity or sensor performance would be determined in prevalence by the fluorogenic fragment, when the latter does not interact covalently with the target species. This is the case for many metal cation sensors that feature anthracenyl derivatives of aza−oxa macrocyclic ligands in which the fluorescence emission is determined by a photoinduced electron transfer (PET) process between the anthracene fragment and the tertiary nitrogen atom of the macrocyclic moiety.[12,15,22]

The main strategy in the design of selective fluorescent chemosensors of this type commonly involves modeling of the structure of the receptor units so as to better match the binding properties of the target metal cation; however, it must not be forgotten that the selectivity and sensitivity of a fluorescent chemosensor are properties of the supramolecular system as a whole in the medium chosen for the host−guest interaction and cannot be completely compartmentalized.

Macrocyclic receptors represent the first choice as receptor moieties for metal cations because of the extensive possibilities that they can offer for the structural modulation of the topology and nature of the binding domain (i.e., by changing the number, nature, and disposition of the donor atoms, cavity size, and conformational flexibility), thus providing an easy route to achieving strong and possibly selective interactions with the substrate of interest. Many of the reported fluoroionophores feature polyoxa-, polyaza-, and aza/oxamacrocycles as the guest binding site (receptors units),[12−22] whereas relatively few examples are reported of fluorescent molecular sensors for metal cations comprising S-donor macrocycles as the binding site.[23−26] The potential of mixed N/S- and N/S/O-donating macrocyclic sites as receptors in fluorescent molecular sensors remains practically untapped and is not considered systematically, despite the fact that the presence of soft donor atoms such as sulfur in the receptor unit would improve the affinity toward heavy-metal ions (Cd, Hg, and Pb) of the resulting chemosensor. Indeed, it is only in the past few years that chemists working in the field have started considering with more attention the option of using mixed-donor sulfur-containing macrocyclic ligands in the construction of fluorescent chemosensors for toxic metal ions, in particular mercury, able to perform mainly in aqueous solution.[27−32]

In this paper, we report on the interaction between the new four aza(oxa)thiamacrocyclic ligand derivatives **L1**−**L4**

(8) (a) Reddy, M. L. P.; Francis, T. *Solvent Extr. Ion Exch.* **2001**, *19*, 839 and references cited therein. (b) Baumann, T. F.; Reynolds, J. G. *Chem. Commun.* **1998**, *16*, 1637. (c) Nelson, A. J.; Reynolds, J. G.; Baumann, T. F.; Fox, G. A. *Appl. Surf. Sci.* **2000**, *167*, 205. (d) Baumann, T. F.; Reynolds, J. G.; Fox, G. A. *React. Funct. Polym.* **2000**, *44*, 111.

(9) (a) Nolan, E. M.; Lippard, S. J. *Chem. Rev.* **2008**, *108*, 3443. (b) Kao, T.-L.; Wang, C.-C.; Pan, Y.-T.; Shiao, Y.-J.; Yen, J.-Y.; Shu, C.-L.; Lee, G.-H.; Peng, S.-M.; Chung, W.-S. *J. Org. Chem.* **2005**, *70*, 2912 and references cited therein. (c) Martínez-Máñez, R.; Espinosa, A.; Tárraga, A.; Molina, P. *Org. Lett.* **2005**, *26*, 5869.

(10) (a) Yang, Y. K.; Yook, K. J.; Tae, J. *J. Am. Chem. Soc.* **2005**, *127*, 16760. (b) Zhang, G.; Zhang, D.; Yin, S.; Yang, X.; Shuai, Z.; Zhu, D. *Chem. Commun.* **2005**, *16*, 2161. (c) Guo, X.; Qian, X.; Jia, L. *J. Am. Chem. Soc.* **2004**, *126*, 2272. (d) Nolan, E. M.; Lippard, S. J. *J. Am. Chem. Soc.* **2003**, *125*, 14270. (e) Hennrich, G.; Walther, W.; Resch-Genger, U.; Sonnenshein, H. *Inorg. Chem.* **2001**, *40*, 641. (f) Zhao, Y.; Lin, Z.; He, C.; Wu, H.; Duan, C. *Inorg. Chem.* **2006**, *45*, 10013. (g) Shamsipur, M.; Hosseini, M.; Alixadeh, K.; Alizadeh, N.; Yari, A.; Caltagirone, C.; Lippolis, V. *Anal. Chim. Acta* **2005**, *353*, 17. (h) Goretzki, G.; Bonnesen, P. V.; Dabestain, R.; Brown, G. M. *ACS Symp. Ser.* **2008**, *943*, 13. (i) Al-Kady, A. S.; Gaber, M.; Hussein, M. M.; Ebeid, E. Z. M. *J. Phys. Chem. A* **2009**, *34*, 9474. (j) Lee, Y. J.; Seo, D.; Kwom, J. Y.; Son, G.; Park, M. S.; Choi, Y.-H.; Soh, J. H.; Lee, H. N.; Lee, K. D.; Yoon, J. *Tetrahedron* **2006**, *62*, 12340. (k) Lee, H. N.; Kim, H. N.; Swamy, K. M. K.; Park, M. S.; Kim, J.; Lee, H.; Lee, H.-H.; Park, S.; Yoon, J. *Tetrahedron Lett.* **2008**, *49*, 1261.

(11) (a) Ko, S. K.; Yang, Y. K.; Tae, J.; Shin, I. *J. Am. Chem. Soc.* **2006**, *128*, 14150. (b) Yang, H.; Zho, Z.; Huang, K.; Yu, M.; Li, F.; Yi, T.; Huang, C. *Org. Lett.* **2007**, *9*, 4729. (c) Yang, Y. K..; Ko, S. K.; Shin, I.; Tae, J. *Org. Biomol. Chem.* **2009**, *7*, 4590.

(12) de Silva, A. P.; Gunaratne, H. Q. N.; Gunnlaugsson, T.; Huxley, A. J. M.; McCoy, C. P.; Rademacher, J. T.; Rice, T. E. *Chem. Rev.* **1997**, *97*, 1515.

(13) Special Issue on Luminescent Sensors: Fabbrizzi, L., Guest Ed. *Coord. Chem. Rev.* **2000**, *205*, 1−232.

(14) Special Issue on Chemical Sensors: Ellis, A. B., Walt, D. R., Guest Eds. *Chem. Rev.*, **2000**, *100*, 2477−2738.

(15) Rurack, K. *Spectrochim. Acta, Part A* **2001**, *57*, 2161.

(16) Fabbrizzi, L.; Licchelli, M.; Taglietti, A. *J. Chem. Soc., Dalton Trans.* **2003**, 3471.

(17) Bell, W. T.; Hext, N. M. *Chem. Soc. Rev.* **2004**, *33*, 589.

(18) Prodi, L. *New J. Chem.* **2005**, *29*, 20.

(19) Special Issue on Fluorescent Sensors. de Silva, A. P., Tecilla, P., Guest Eds. *J. Mater. Chem.* **2005**, *15*, 2617−2976.

(20) Amendola, V.; Fabbrizzi, L.; Foti, F.; Licchelli, M.; Mangano, C.; Pallavicini, P.; Poggi, A.; Sacchi, D.; Taglietti, A. *Coord. Chem. Rev.* **2006**, *250*, 273.

(21) Basade-Desmonts, L.; Reinhoudt, D. N.; Crego-Calama, M. *Chem. Soc. Rev.* **2007**, *36*, 993.

(22) (a) Lodeiro, C.; Pina, F. *Coord. Chem. Rev.* **2009**, *253*, 1353. (b) Lodeiro, C.; Capelo, J. L.; Mejuto, J. C.; Oliveira, E.; Santos, H. M.; Pedras, B.; Nuñez, C. *Chem. Soc. Rev.* **2010**, *39*, 2948.

(23) Bronson, R. T.; Bradshaw, J. S.; Savage, P. B.; Fuangswasdi, S.; Lee, S. C.; Krakowiak, K. E.; Izatt, R. M. *J. Org. Chem.* **2001**, *66*, 4752.

(24) Lee, S. C.; Izatt, R. M.; Zhang, X. X.; Nelson, E. G.; Lamb, J. D.; Savage, P. B.; Bradshaw, J. B. *Inorg. Chim. Acta* **2001**, *317*, 174.

(25) (a) De Santis, G.; Fabbrizzi, L.; Lichelli, M.; Mangano, C.; Sacchi, D.; Sardone, N. *Inorg. Chim. Acta* **1997**, *257*, 69. (b) Yoon, S.; Miller, E. W.; He, Q.; Do, P. H.; Chang, C. J. *Angew. Chem., Int. Ed.* **2007**, *46*, 6658.

(26) (a) Blake, A. J.; Bencini, A.; Caltagirone, C.; De Filippo, G.; Dolci, L. S.; Garau, A.; Isaia, F.; Lippolis, V.; Mariani, P.; Prodi, L.; Montalti, M.; Zaccheroni, N.; Wilson, W. *Dalton Trans.* **2004**, 2771. (b) Aragoni, M. C.; Arca, M.; Bencini, A.; Blake, A. J.; Caltagirone, C.; Decortes, A.; Demartin, F.; Devillanova, F. A.; Faggi, E.; Dolci, L. S.; Garau, A.; Isaia, F.; Lippolis, V.; Prodi, L.; Wilson, W.; Valtancoli, B.; Zaccheroni, N. *Dalton Trans.* **2005**, 2994. (c) Tamayo, A.; Pedras, B.; Lodeiro, C.; Escriche, L.; Casabó, J.; Capelo, J. L.; Covelo, B.; Kivekas, R.; Sillanpää, R. *Inorg. Chem.* **2007**, *46*, 7818.

(27) (a) Jiménez, D.; Martínez-Máñez, R.; Sancenón, F.; Soto, J. *Tetrahedron Lett.* **2004**, *45*, 1257. (b) Ros-Lis, J. V.; Martínez-Máñez, R.; Rurack, K.; Sancenón, F.; Soto, J.; Spieles, M. *Inorg. Chem.* **2004**, *43*, 5183. (c) Descazo, A. B.; Martínez-Máñez, R.; Redeglia, R.; Rurack, K.; Soto, J. *J. Am. Chem. Soc.* **2003**, *125*, 3418.

(28) (a) Rurack, K.; Trieflinger, C.; Koval'chuck, A.; Daub, J. *Chem.—Eur. J.* **2007**, *13*, 8998. (b) Bricks, J. L.; Kovalchuck, A.; Trieflinger, C.; Nofz, M.; Büschel, M.; Tolmachev, A. I.; Daub, J.; Rurack, K. *J. Am. Chem. Soc.* **2005**, *127*, 13522.

Scheme 1

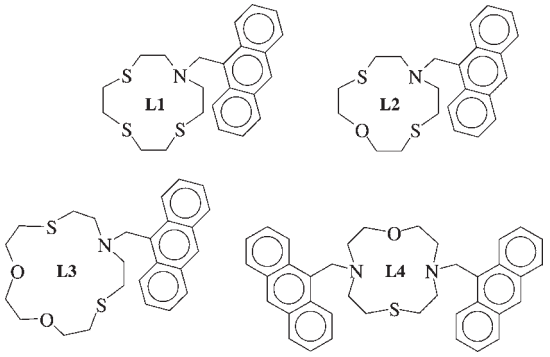

(Scheme 1) and transition- and post-transition-metal ions including the heavy toxic ones Cd^{2+}, Hg^{2+}, and Pb^{2+}, with the aim of testing the effects of the different mixed-donor macrocyclic binding domains (all containing at least two sulfur atoms) on the optical response to metal ions of the common anthracenyl signaling core, in the quest for fluorescent probes for mercury(II) detection in small samples. Spectrophotometric and spectrofluorimetric titrations of the four ligands with the metal ions considered were initially performed in 1:1 (v/v) MeCN/H_2O solutions. Additionally, the interaction of Hg^{2+} with **L1**−**L4** in 1:1 (v/v) MeCN/H_2O solutions was studied by fluorimetric techniques in microsamples in order to explore the potential use of these ligands as mercury(II) molecular probes in small environments. Gas-phase studies were also performed using the ligands as potential matrix-assisted laser desorption/ionization time-of-flight mass spectrometry (MALDI-TOF-MS) matrixes for metal detection.

Experimental Section

Instruments and Materials. All of the syntheses of the ligands were carried out using standard Schlenk techniques. Solvents were dried by conventional methods and distilled under N_2(g) before use. Elemental analysis was performed using a Thermo-Finnigan CE Flash-EA 1112-CHNS instrument provided by the Chemical Analysis Service of the REQUIMTE, DQ, Universidade Nova de Lisboa, Monte de Caparica, Portugal. ^{1}H and ^{13}C NMR spectra were recorded on a Varian VXR400 spectrometer.

MALDI-TOF-MS spectra and titrations have been performed in a MALDI-TOF-MS model Voyager DE-PRO Biospectrometry Workstation equipped with a nitrogen laser radiating at 337 nm from Applied Biosystems (Foster City, CA) from the MALDI-TOF-MS Service of the REQUIMTE, Chemistry Department, Universidade Nova de Lisboa, and in the MALDI-TOF-MS-MS model 4700 Applied Biosystems at the Faculty of Science of Ourense, University of Vigo, Ourense, Spain. The acceleration voltage was 2.0×10^4 kV with a delayed extraction time of 200 ns. The spectra represent accumulations of 5×100 laser shots. The reflection mode was used. The ion source and flight tube pressures were less than 1.80×10^{-7} and 5.60×10^{-8} Torr, respectively.

The MALDI-MS spectra of the soluble ligand (1 or 2 μg μL^{-1}) were recorded using the conventional sample preparation method for MALDI-MS without other MALDI matrixes. In the metal titrations by MALDI, 1 μL of a 1:1 (v/v) MeCN/H_2O solution containing the ligand and metal in a 1:1 molar ratio was put on the sample holder as mentioned above. The sample holder was inserted into the ion source. Chemical reaction between the ligand and metal salts occurred in the holder, and complex species were produced in the gas phase.

Organic reagents and transition-metal salts were purchased from Sigma-Aldrich and used as received. Precursor macrocyclic compounds 1-aza-4,7,10-trithiacyclododecane ([12]aneNS$_3$), 1-aza-4,10-dithia-7-oxacyclododecane ([12]aneNS$_2$O), 1-aza-4,13-dithia-7,10-dioxacyclopentadecane ([15]aneNS$_2$O$_2$), and 1,7-diaza-4-thia-10-oxacyclododecane ([12]aneN$_2$SO) were prepared as reported in the literature.[33]

Spectrophotometric and Spectrofluorimetric Measurements. Absorption spectra were recorded on a Perkin-Elmer Lambda 35 spectrophotometer and fluorescence emission on a Perkin-Elmer LS45 spectrofluorimeter. The linearity of the fluorescence emission versus the concentration was checked in the concentration range used (10^{-4}−10^{-6} M). A correction for the absorbed light was performed when necessary.[34] All spectrofluorimetric titrations were performed as follows: the stock solutions of the ligands (ca. 1×10^{-4} M) were prepared by dissolving an appropriate amount of the ligands in a 50 mL volumetric flask and diluting to the mark with CH_3CN UVA-sol. The titration solutions ([**L1**] = 1.63×10^{-5} M or 1.70×10^{-5} M, [**L2**] = 1.42×10^{-5} M or 1.50×10^{-5} M, [**L3**] = 1.61×10^{-5} M, [**L4**] = 0.82×10^{-5} M or 1.35×10^{-4} M) were prepared by the appropriate dilution of the stock solutions in a final 1:1 (v/v) MeCN/H_2O solvent mixture. The pH of the solution of each ligand was checked before titration. Titrations of the ligands were carried out by the addition of microliter amounts of standard solutions of the metal ions in acetonitrile or Millipore-grade water. The absorbance and emission of these solutions were read after each addition (λ_{exc} = 367 nm and λ_{em} = 417 nm for **L1**, λ_{exc} = 367 nm and λ_{em} = 422 nm for **L2**, λ_{exc} = 367 nm and λ_{em} = 414 nm for **L3**, and λ_{exc} = 367 nm and λ_{em} = 415 nm for **L4**). The stock solutions of each metal ion of NaOH and HBF_4 (ca. 1×10^{-4} M) were prepared by dissolving an appropriate amount of the salt in a 10 mL volumetric flask and diluting to the mark with the appropriate solvent (MeCN or H_2O). Luminescence quantum yields were measured using a solution of sublimed anthracene in cyclohexane as the standard [Φ_F = 0.36].[34]

Emission spectra of **L1**−**L4** and of the respective **L**/Hg^{2+} mixtures in a 1:1 molar ratio were recorded as microliter samples using a NANODROP N1000 spectrophotometer and a NANODROP N3300 spectrofluorimeter from Thermo-Scientific.[35] Between 1 and 2 μL of the solution in 1:1 (v/v) MeCN/H_2O of each sample [ligands or ligand/mercury(II) mixtures] was placed on the optical pedestal, and the sample was drawn into a column and measured.

The solid-state emission spectra of **L1**−**L4** were recorded on a Horiba-Yvon-Spex Fluoromax-4 spectrofluorimeter using an external fiber-optic device.

(29) (a) Li, M.-J.; Chu, B. W.-K.; Zhu, N.; Yam, V. W.-W. *Inorg. Chem.* **2007**, *46*, 720. (b) Li, M.-J.; Ko, C.-C.; Duan, G.-P.; Zhu, N.; Yam, V. W.-W. *Organometallics* **2007**, *26*, 6091.

(30) Mameli, M.; Arca, M.; Caltagirone, C.; Demartin, F.; De Filippo, G.; Devillanova, F. A.; Garau, A.; Isaia, F.; Lippolis, V.; Murgia, S.; Prodi, L.; Pintus, A.; Zaccheroni, N. *Chem.—Eur. J.* **2010**, *16*, 919.

(31) Yoon, S.; Albers, A. E.; Wong, A. P.; Chang, C. J. *J. Am. Chem. Soc.* **2005**, *127*, 16030.

(32) (a) Yuan, M.; Li, Y.; Li, J.; Li, C.; Liu, X.; Lv, J.; Xu, J.; Liu, H.; Wang, S.; Zhu, D. *Org. Lett.* **2007**, *9*, 2313. (b) Ho, M.-L.; Chen, K.-Y.; Lee, G.-H.; Chen, Y.-C.; Wang, C.-C.; Lee, J.-F.; Chung, W.-C.; Chou, P.-T. *Inorg. Chem.* **2009**, *48*, 10304.

(33) (a) Caltagirone, C.; Bencini, A.; Demartin, F.; Devillanova, F. A.; Garau, A.; Isaia, F.; Lippolis, V.; Papke, U.; Tei, L.; Verani, G. *Dalton Trans.* **2003**, *5*, 901. (b) van de Water, L. G. A.; Buijs, W.; Driessen, W. L.; Reedijk, J. *New J. Chem.* **2001**, *25*, 243. (c) Afshar, S.; Marcus, S. T.; Gahan, L. R.; Hambley, T. W. *Aust. J. Chem.* **1999**, *52*, 1.

(34) (a) Berlman, I. B. *Handbook of Fluorescence Spectra of Aromatic Molecules*, 2nd ed.; Academic Press: New York, 1971. (b) Montalti, L.; Credi, A.; Prodi, T.; Gandolfi, M. T. *Handbook of Photochemistry*, 3rd ed.; Taylor and Francis Group: Boca Ratón, FL, 2006. (c) Credi, A.; Prodi, L. *Spectrochim. Acta* **1998**, *54*, 159.

(35) http://www.nanodrop.com/Default.aspx (Last entrance: April 16, 2010).

Density Functional Theory (DFT) Calculations. DFT in the Kohn−Sham approximation was used to optimize the geometry of all of the species modeled. The B3LYP exchange-correlation functional was used throughout all of the calculations with the 6-31G* basis set for every atom except mercury,[36] for which the LANL2DZ electron core potential was used, together with the corresponding LANL2DZ basis set.[37] The stabilities of the wave function and the Hessian were calculated on the optimized geometries at the same level to establish that both the optimized geometry and the optimized wave function correspond to a minimum.

All of the calculations have been performed using the *Gaussian03* suite of programs.[38]

Synthesis of 1-(9-Anthracenylmethyl)-1-aza-4,7,10-trithiacyclododecane (L1). A solution of 9-(chloromethyl)anthracene (0.203 g, 0.896 mmol) in anhydrous MeCN (40 mL) was added dropwise to a mixture of [12]aneNS$_3$ (0.2 g, 0.896 mmol) and K_2CO_3 (0.74 g, 5.38 mmol) in anhydrous MeCN (50 mL). This mixture was stirred at room temperature for 1 week under N_2. The solid was filtered off, and the solvent was removed under reduced pressure. The residue was dissolved in $CHCl_3$ and washed with H_2O. The organic phase was dried over Na_2SO_4, and the solvent was evaporated under reduced pressure to afford a yellow solid (98% yield). Elem anal. Found (calcd for $C_{23}H_{27}NS_3 + 1.5H_2O$): C, 62.65 (62.69); H, 6.84 (6.86); N, 3.19 (3.18); S, 21.80 (21.83). ^{1}H NMR (300 MHz, $CDCl_3$): δ 2.53 (br s, 5H,), 2.73 (s, 6H), 2.88 (s, 5H), 4.59 (s, 2H) 7.43−7.49 (m, 3H), 7.76−7.79 (m, 1H), 7.97 (d, J = 9 Hz, 2H), 8.28−8.30 (m, 1H), 8.41−8.45 (m, 2H). ^{13}C NMR (100 MHz, $CDCl_3$): δ 26.29, 27.97, 28.72, 51.52, 52.22, 124.74, 124.87, 125.78, 127.85, 129.08, 129.35, 130.80, 131.37 MALDI-TOF-MS: m/z 414.09 [**L1** + H]$^+$. UV−vis [1:1 (v/v) MeCN/H_2O; λ_{max}, nm (ε_{max}, dm^3 mol^{-1} cm^{-1})]: 317 (2000), 332 (2600), 349 (3700), 367 (5000), 387 (4600).

Synthesis of 1-(9-Anthracenylmethyl)-1-aza-4,10-dithia-7-oxacyclododecane (L2). A solution of 9-(chloromethyl)anthracene (0.220 g, 0.966 mmol) in anhydrous MeCN (50 mL) was added dropwise to a mixture of [12]aneNS$_2$O (0.2 g, 0.966 mmol) and K_2CO_3 (0.8 g, 5.77 mmol) in anhydrous MeCN (50 mL). This mixture was stirred at room temperature for 1 week under N_2. The solid was filtered off, and the solvent was removed under reduced pressure. The residue was dissolved in $CHCl_3$ and washed with H_2O. The organic phase was dried over Na_2SO_4, and the solvent was evaporated under reduced pressure to afford a yellow solid (93% yield). Elem anal. Found (calcd for $C_{23}H_{27}NOS_2 + 2.5H_2O$): C, 62.45 (62.41); H, 7.27 (7.29); N, 3.15 (3.16); S, 14.46 (14.49). ^{1}H NMR (300 MHz, $CDCl_3$): δ 2.72−3.16 (m, 16H), 3.80 (s, 2H), 7.44−7.54 (m, 3H), 7.80−7.83 (m, 1H), 8.00 (d, J = 8.1 Hz, 1H), 8.31−8.34 (m, 1H), 8.43−8.51 (m, 3H). ^{13}C NMR (75.42 MHz, $CDCl_3$): δ 28.01, 30.37, 51.32, 51.37, 74.40, 124.71, 124.81, 125.54, 126.79, 127.43, 128.85, 131.12, 131.20. MALDI-TOF-MS: m/z 398.20 [**L2** + H]$^+$. UV−vis [1:1 (v/v) MeCN/H_2O; λ_{max}, nm (ε_{max}, dm^3 mol^{-1} cm^{-1})]: 318 (2100), 333 (3000), 349 (4900), 367 (6900), 387 (6300).

Synthesis of 1-(9-Anthracenylmethyl)-1-aza-4,13-dithia-7,10-dioxacyclopentadecane (L3). A solution of 9-(chloromethyl)-anthracene (0.105 g, 0.795 mmol) in anhydrous MeCN (50 mL) was added dropwise to a mixture of [15]aneNS$_2$O$_2$ (0.2 g, 0.795 mmol) and K_2CO_3 (0.74 g, 5.38 mmol) in anhydrous MeCN (50 mL). This mixture was stirred at room temperature for 1 week under N_2. The solid was filtered off, and the solvent was removed under reduced pressure. The residue was dissolved in $CHCl_3$ and washed with H_2O. The organic phase was dried over Na_2SO_4, and the solvent was evaporated under reduced pressure to afford a yellow solid (89% yield). Elem anal. Found (calcd for $C_{25}H_{31}NO_2S_2 + 0.5H_2O$): C, 66.77 (66.63); H, 7.14 (7.16); N, 3.10 (3.11); S, 14.20 (14.23). ^{1}H NMR (300 MHz, $CDCl_3$): δ 2.66 (t, J = 10.5 Hz, 4H), 2.89 (br s, 9H), 3.63−3.75 (m, 9H), 7.45−7.64 (m, 3H), 7.79−7.82 (m, 1H), 7.99−8.05 (m, 2H), 8.32 (d, J = 9 Hz, 1H), 8.67 (d, J = 9 Hz, 2H). ^{13}C NMR (75.42 MHz, $CDCl_3$): δ 30.25, 31.31, 50.90, 54.22, 70.91, 73.55, 124.91, 125.07, 125.31, 127.00, 127.73, 129.09, 129.38, 131.48. MALDI-TOF-MS: m/z 442.16 [**L3** + H]$^+$. UV−vis [1:1 (v/v) MeCN/H_2O; λ_{max}, nm (ε_{max}, dm^3 mol^{-1} cm^{-1})]: 319 (2000), 332 (3100), 349 (5400), 367 (7500), 387 (6600).

Synthesis of 1−7-Bis(9-anthracenylmethyl)-1,7-diaza-4-thia-10-oxacyclododecane (L4). A solution of [12]aneN$_2$SO (0.1 g, 0.525 mmol) in dry MeCN (25 mL) was added dropwise to a mixture of 9-(chloromethyl)anthracene (0.238 g, 1.05 mmol) and K_2CO_3 (0.73 g, 5.25 mmol) in dry MeCN (25 mL). The mixture was refluxed for 24 h under N_2. The solid was filtered off, and the solvent was removed under reduced pressure. The residue obtained (yellow oil) was purified by flash chromatography (alumina gel, 1:1 CH_2Cl_2/MeOH) to afford a brown solid (59.8% yield). Elem anal. Found (calcd for $C_{38}H_{38}N_2O_1S + 1.5H_2O$): C, 76.15 (76.35); H, 6.89 (6.91); N, 4.70 (4.69); S, 5.35 (5.36). ^{1}H NMR (300 MHz, $CDCl_3$): δ 2.69−2.78 (m, 8H), 3.15 (br s, 8H), 4.58 (s, 4H), 7.41−7.51 (m, 8H), 7.97 (d, J = 8.1 Hz, 2H), 7.38−7.45 (m, 8H). ^{13}C NMR (75.42 MHz, $CDCl_3$): δ 26.55, 29.32, 52.41, 56.85, 71.53, 124.94, 125.13, 125.66, 127.27, 127.65, 129.10, 131.35, 131−50. MALDI-TOF-MS: m/z 371.32 [**L4** + H]$^+$. UV−vis [1:1 (v/v) MeCN/H_2O; λ_{max}, nm (ε_{max}, dm^3 mol^{-1} cm^{-1})]: 317 (3500), 332 (4900), 349 (7900), 367 (11 400), 387 (10 800).

Results and Discussion

Photophysical Properties and Metal-Ion Binding Studies. An aliphatic amine group, when bonded to emissive chromophores, usually causes the quenching of their fluorescence emission intensity via a PET quenching process.[12,39,40] This particular property opens the possibility of signaling the presence of metal cations, both in solution and in the gas phase by linking, via an aliphatic amine group, an appropriate receptor unit to a fluorogenic fragment in a *conjugated* fluorescent chemosensor.

In fact, when metal ions coordinate to the nitrogen atom(s) in these systems, two different behaviors can be observed: (i) if the metal is a d^{10} ion, an enhancement on the fluorescence intensity (CHEF effect) is normally

(36) (a) Becke, A. D. *J. Chem. Phys.* **1993**, *98*, 5648. (b) Lee, W.; Yang, R. G.; Parr, R. G. *Phys. Rev. B* **1988**, *37*, 785.
(37) Hay, P. J.; Wadt, W. R. *J. Chem. Phys.* **1985**, *82*, 270.
(38) Frisch, M. J.; Trucks, G. W.; Schlegel, H. B.; Scuseria, G. E.; Robb, M. A.; Cheeseman, J. R.; Montgomery, J. A., Jr.; Vreven, T.; Kudin, K. N.; Burant, J. C.; Millam, J. M.; Iyengar, S. S.; Tomasi, J.; Barone, V.; Mennucci, B.; Cossi, M.; Scalmani, G.; Rega, N.; Petersson, G. A.; Nakatsuji, H.; Hada, M.; Ehara, M.; Toyota, K.; Fukuda, R.; Hasegawa, J.; Ishida, M.; Nakajima, T.; Honda, Y.; Kitao, O.; Nakai, H.; Klene, M.; Li, X.; Knox, J. E.; Hratchian, H. P.; Cross, J. B.; Bakken, V.; Adamo, C.; Jaramillo, J.; Gomperts, R.; Stratmann, R. E.; Yazyev, O.; Austin, A. J.; Cammi, R.; Pomelli, C.; Ochterski, J. W.; Ayala, P. Y.; Morokuma, K.; Voth, G. A.; Salvador, P.; Dannenberg, J. J.; Zakrzewski, V. G.; Dapprich, S.; Daniels, A. D.; Strain, M. C.; Farkas, O.; Malick, D. K.; Rabuck, A. D.; Raghavachari, K.; Foresman, J. B.; Ortiz, J. V.; Cui, Q.; Baboul, A. G.; Clifford, S.; Cioslowski, J.; Stefanov, B. B.; Liu, G.; Liashenko, A.; Piskorz, P.; Komaromi, I.; Martin, R. L.; Fox, D. J.; Keith, T.; Al-Laham, M. A.; Peng, C. Y.; Nanayakkara, A.; Challacombe, M.; Gill, P. M. W.; Johnson, B.; Chen, W.; Wong, M. W.; Gonzalez, C.; Pople, J. A. *Gaussian03*, revision C.02; Gaussian, Inc.: Wallingford, CT, 2004.
(39) Bissel, R. A.; de Silva, A. P.; Gunaratne, H. Q. N.; Lynch, P. L. M.; Maguire, G. E. M.; McCoy, C. P.; Sandanayake, K. R. A. S. *Top. Curr. Chem.* **1993**, *168*, 223.
(40) (a) Albelda, M. T.; Díaz, P.; García-España, E.; Lima, J. C.; Lodeiro, C.; de Melo, J. S.; Parola, A. J.; Pina, F.; Soriano, C. *Chem. Phys. Lett.* **2002**, *353*, 63. (b) de Melo, J. S.; Pina, J.; Pina, F.; Lodeiro, C.; Parola, A. J.; Lima, J. C.; Albelda, M. T.; Clares, M. P.; García-España, E.; Soriano, C. *J. Phys. Chem. A* **2003**, *107*, 11307. (c) de Melo, J. S.; Albelda, M. T.; Díaz, P.; Garcia-España, E.; Lodeiro, C.; Alves, S.; Lima, J. C.; Pina, F.; Soriano, C. *J. Chem. Soc., Perkin Trans. 2* **2002**, 991.

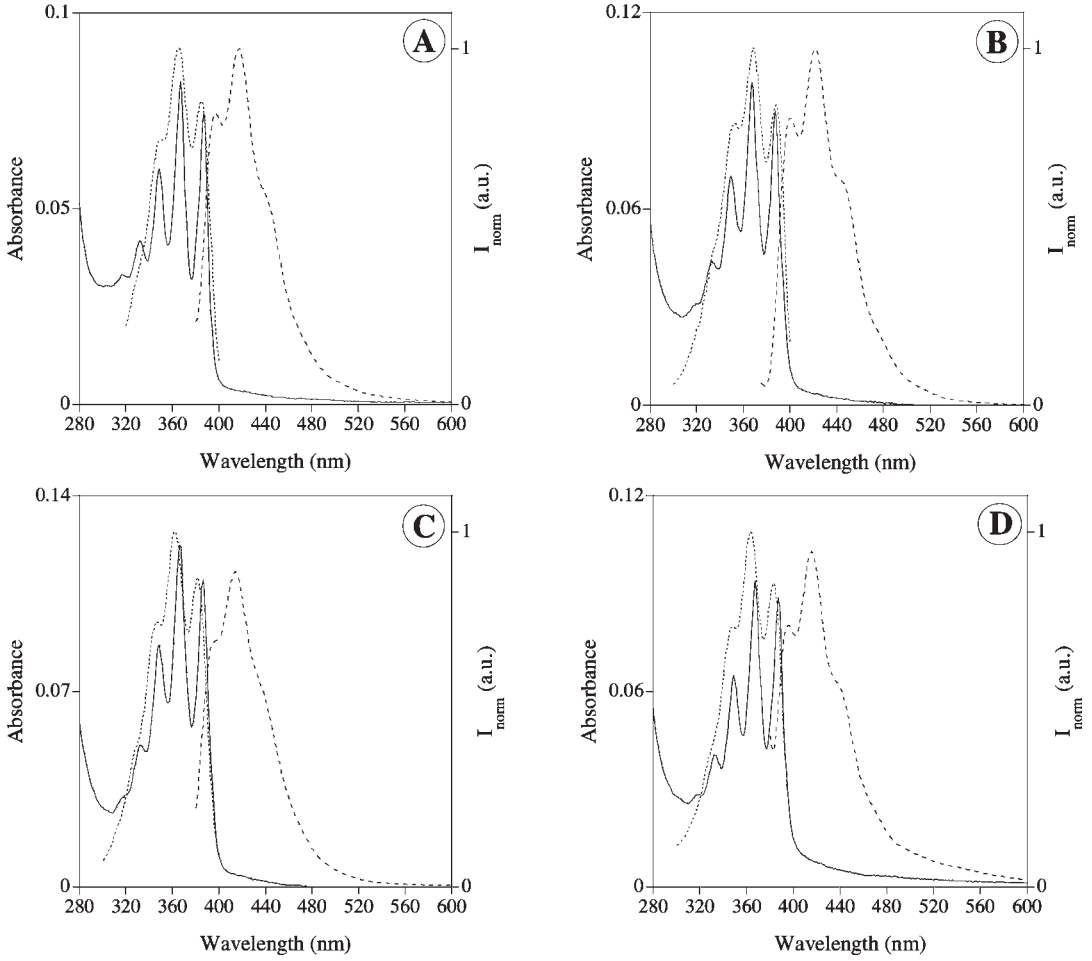

Figure 1. Absorption (full line), emission (broken line), and excitation spectra (dotted line) of **L1**−**L4**: **L1** (A) (1.63×10^{-5} M; λ_{exc} = 367 nm; λ_{em} = 417 nm); **L2** (B) (1.42×10^{-5} M; λ_{exc} = 367 nm; λ_{em} = 422 nm); **L3** (C) (1.61×10^{-5} M; λ_{exc} = 367 nm; λ_{em} = 414 nm); **L4** (D) (0.82×10^{-5} M; λ_{exc} = 367 nm; λ_{em} = 415 nm), in 1:1 (v/v) $MeCN/H_2O$ at room temperature.

observed, especially for metal ions such as Cd^{2+}, Ag^{+}, Cu^{+}, or Zn^{2+}; (ii) if the metal is a $d^{<10}$ ion, a quenching effect (CHEQ) can be expected via enhancement of the spin−orbit coupling due to heavy-atom effects or PET processes.[41] Even if Hg^{2+} is a d^{10} ion, it is more common to find fluorescent molecular systems based on the CHEQ effect because of the heavy-atom effect.

Anthracene and highly π-delocalized aromatic systems have extensively been used in the construction of fluorescent chemosensors for metal ions based on the PET transduction mechanism, which, as mentioned above, are characterized by an intrinsic supramolecular nature because each component of the molecular system performs one of the necessary functions.[12,39,42] The great success of anthracene-based chemosensors can be attributed to the fact that the receptor design for metal ions is relatively rational. In fact, anthracene has been paired with a variety of receptors including polyazacycloalkanes and azacrown ethers to afford fluorescent chemosensors selective for transition-metal ions or alkaline metals depending on the "hard/soft" nature of the receptor donor set. Anthracene-based chemosensors featuring sulfur-containing macrocyclic ligands as receptor units have nearly been considered. Therefore, we wanted to study the potentialities of these kinds of cyclic receptors in conjunction with anthracene in signaling heavy-metal ions following a PET transduction mechanism.

The absorption, emission, and excitation emission spectra of **L1**−**L4** in 1:1 (v/v) $MeCN/H_2O$ solutions at room temperature are reported in Figure 1.

The absorption spectra show the characteristic bands of the anthracene derivatives between 320 and 400 nm. All spectra feature a vibrational fine structure with the four typical maxima for anthracene systems. The excitation spectra for all ligands were obtained with λ_{em} at 417 (**L1**), 422 (**L2**), 414 (**L3**), and 415 (**L4**) nm. In all cases, these spectra were coincident with the absorption spectra. In Figure 2, the spectra after protonation with an aqueous solution of HBF_4 are collected. There we can see that the absorption spectra of the ligands were practically unaffected by protonation. However, upon the addition of acid (HBF_4 and H_2O solution), an increase in the emission

(41) (a) McClure, D. S. *J. Chem. Phys.* **1952**, *20*, 682. (b) Burress, C. N.; Bodine, M. I.; Elbjeirami, O.; Reibenspies, J. H.; Omary, M. A.; Gabbaie, F. P. *Inorg. Chem.* **2007**, *46*, 1388.

(42) (a) Bianchi, A.; Berni, E.; Bencini, A.; Fornasari, P.; Giorgi, C.; Lima, J. C.; Lodeiro, C.; Melo, M. J.; Parola, A. J.; Pina, F.; Valtancoli, B. *Dalton Trans.* **2004**, *14*, 2180. (b) Aragoni, M. C. M.; Arca, M.; Bencini, A.; Blake, A. J.; Caltagirone, C.; De Filippo, G.; Devillanova, F. A.; Garau, A.; Gelbrich, T.; Hurthouse, M. B.; Isaia, F.; Lippolis, V.; Mameli, M.; Mariani, P.; Valtancoli, B.; Wilson, C. *Inorg. Chem.* **2007**, *46*(11), 4548. (c) Tamayo, A.; Oliveira, E.; Covelo, B.; Casabó, J.; Escriche, L.; Lodeiro, C. *Z. Anorg. Allg, Chem.* **2007**, *633*, 1809.

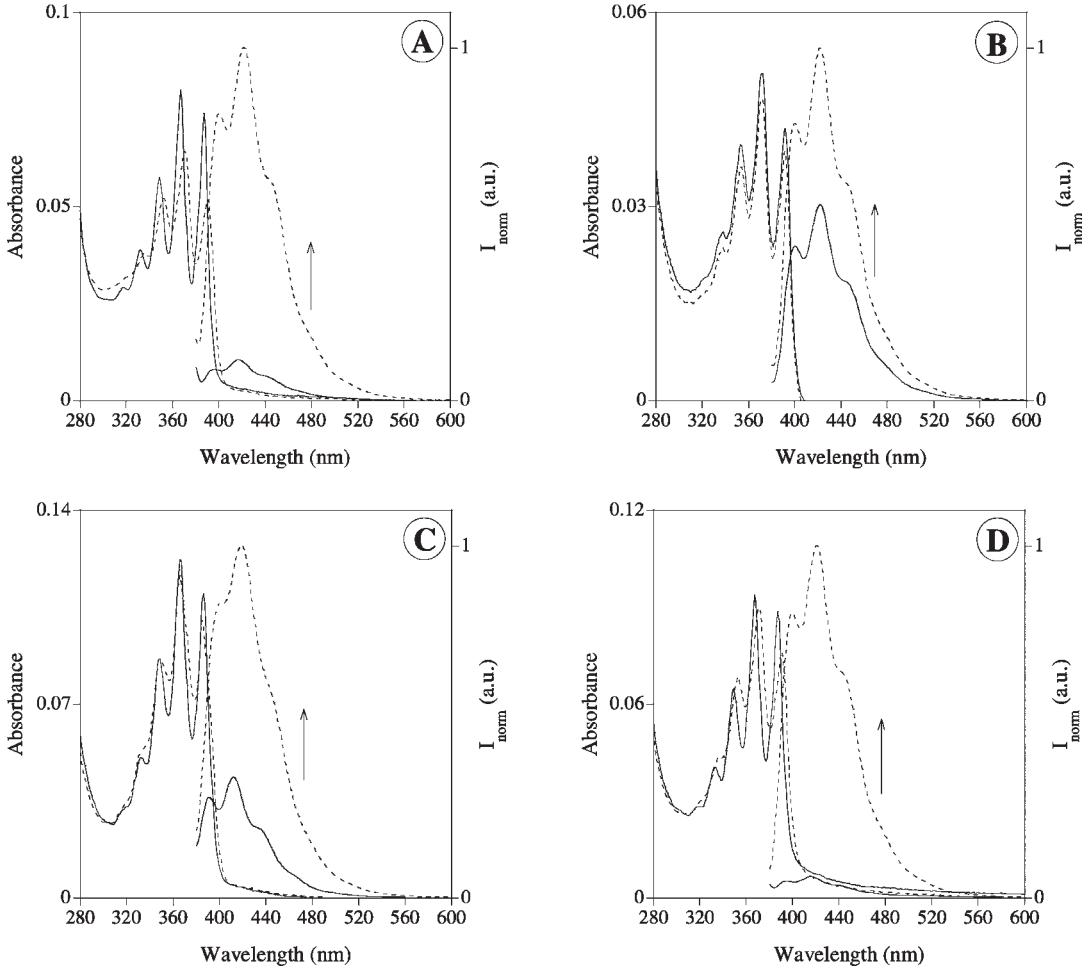

Figure 2. Absorption and normalized emission spectra of **L1**−**L4**. The full lines represent the free ligands, and the dotted lines represent the spectra obtained after the addition of 1 equiv of HBF_4 (H_2O solution) to a 1:1 (v/v) $MeCN/H_2O$ solution of the ligands. The initial solutions of the ligands had pH values of 6.70 (**L1**), 6.69 (**L2**), 6.72 (**L3**), and 6.62 (**L4**); the final solutions after the addition of HBF_4 had pH values of 2.70 (**L1**), 2.19 (**L2**), 2.19 (**L3**), and 2.28 (**L4**). **L1** (A) (1.63×10^{-5} M; $\lambda_{exc} = 367$ nm); **L2** (B) (1.42×10^{-5} M; $\lambda_{exc} = 367$ nm); **L3** (C) (1.61×10^{-5} M; $\lambda_{exc} = 367$ nm); **L4** (D) (0.82×10^{-5} M; $\lambda_{exc} = 367$ nm).

intensity was observed in all cases, reaching a maximum after the addition of 1 equiv of HBF_4. This observation reflects the fact that the protonation process involves the aliphatic amine groups of **L1**−**L4**, thus preventing the PET from the lone pair of electrons on the nitrogen atom(s) to the excited anthracene unit(s). On the other hand, the addition of 1 equiv of NaOH (H_2O solution) to a 1:1 (v/v) $MeCN/H_2O$ solution of the ligands resulted in all cases in the detection of a small quenching effect on the fluorescence intensity (see Figure S1 in the Supporting Information).

Significant changes in the absorption and emission spectra of 1:1 (v/v) $MeCN/H_2O$ solutions of **L1**−**L4** were observed upon the addition of Hg^{2+} salts. Figure 3 shows the changes observed for the absorption spectra of the anthracene-containing macrocycles **L1**−**L4** upon the addition of increasing amounts of $Hg(CF_3SO_3)_2$. The addition of this metal ion causes a red shift of the anthracene bands in the absorption spectra of **L1**, **L2**, and **L4**, while a small decrease of the absorbances is observed for all four ligands; furthermore, a small absorbance increase around 300 nm is also observed. The observed changes on the anthracene bands can be attributed to interactions between the metal ion and the aliphatic nitrogen(s), whereas the changes around 300 nm can be attributed to the involvement of the sulfur atoms in the metal coordination.[43]

Inflection points in the spectrophotometric titrations of **L1**, **L2**, and **L4** with mercury(II) following the absorbance at 367 nm (see the insets in Figure 3A−D) suggest the formation of 1:2 metal-to-ligand complexes in which, very likely, two units of the macrocyclic ligands are coordinated to one metal center in a sandwich manner. In the case of **L3** (see the inset in Figure 3C), changes in the absorption spectra occurred until the addition of 1 equiv of the metal ion. However, spectrophotometric titration curves of **L1**−**L4** with Hg^{2+} could only be fitted according to a 1:2 metal-to-ligand complexation model. Association constants (log $K_{ass.}$) of 11.75(3), 12.02(4), 11.06(1), and 12.75(15) were evaluated for the formation of complexes $[Hg(\mathbf{L1})_2]^{2+}$, $[Hg(\mathbf{L2})_2]^{2+}$, $[Hg(\mathbf{L3})_2]^{2+}$, and $[Hg(\mathbf{L4})_2]^{2+}$, respectively.[44]

(43) (a) Tamayo, A.; Lodeiro, C.; Escriche, L.; Casabó, J.; Covelo, B.; González, P. *Inorg. Chem.* **2005**, *44*, 8105. (b) Tamayo, A.; Casabó, J.; Escriche, L.; Lodeiro, C.; Covelo, B.; Brondino, C. D.; Kikeväs, R.; Sillampää, R. *Inorg. Chem.* **2006**, *45*, 1140. (c) Tamayo, A.; Escriche, L.; Casabó, J.; Covelo, B.; Lodeiro, C. *Eur. J. Inorg. Chem.* **2006**, *15*, 2997.

(44) Spectrophotometric data for the titrations of **L1**−**L4** with Hg^{2+} and spectrofluorimetric data for the titrations of **L1**−**L3** with Hg^{2+} were fitted by using HypSpec: http://www.hyperquad.co.uk/hq2000.htm. (a) Gans, P.; Sabatini, A.; Vacca, A. *Talanta* **1996**, *43*, 1739. (b) Gans, P.; Sabatini, A.; Vacca, A. *Ann. Chim.* **1999**, *89*, 45.

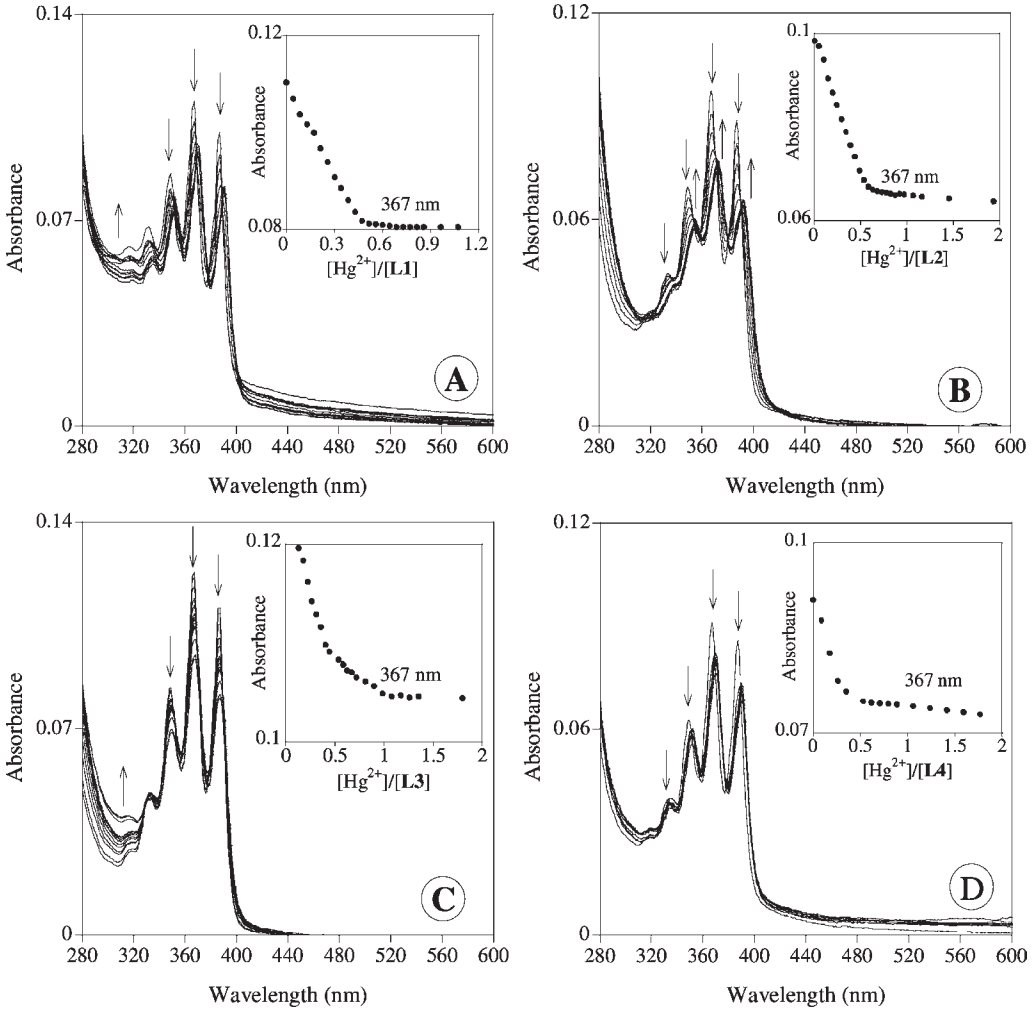

Figure 3. Absorption spectra of 1:1 (v/v) MeCN/H_2O solutions of **L1**−**L4** as a function of increasing amounts of added $Hg(CF_3SO_3)_2$. The insets show changes in the absorbance at 367 nm during the spectrophotometric titrations: **L1** (A) (1.70×10^{-5} M); **L2** (B) (1.50×10^{-5} M); **L3** (C) (1.61×10^{-5} M); **L4** (D) (0.82×10^{-5} M).

This result is also supported by DFT calculations performed in the case of **L2** (see below).

Figure 4 shows the changes observed for the fluorescence emission spectra of **L1**−**L4** upon titrations with $Hg(CF_3SO_3)_2$. From the initial additions of the metal ion to solutions of the ligands in 1:1 (v/v) MeCN/H_2O, the fluorescence intensity emission of the ligands decreases until it reaches a plateau after 0.5 equiv of the metal are added (see the insets in Figure 4). The strongest quenching is observed for **L2** (see Figure 5), while the fluorescence emission intensity of **L4** is practically unaffected by the addition of the metal ion. As stated above, the addition of Hg^{2+} is expected to quench the fluorescence emission of anthracene-based conjugated fluorescent chemosensors via enhancement of the spin−orbit coupling, so as a result of this behavior, ligand **L2** was revealed as the best Hg^{2+} ON−OFF fluorescence probe in its family.

In order to perform a selectivity study, all four ligands were titrated in the same experimental conditions with Zn^{2+}, Cd^{2+}, Pb^{2+}, Cu^{2+}, Ag^{+}, Fe^{2+}, Co^{2+}, Ni^{2+}, Mn^{2+}, Ca^{2+}, Na^{+}, Mg^{2+}, and K^{+}. No significant changes were observed in the absorption spectra of **L1**−**L4** upon the addition of these metal ions. Furthermore, as can be seen in Figure 6, a significant CHEQ effect of the type ON−OFF on the fluorescence emission intensity of the four ligands in 1:1 (v/v) MeCN/H_2O was observed only in the case of **L2** upon the addition of Hg^{2+}; this total quenching observed would permit, therefore, one to distinguish mercury(II) from the other metal ions added, using **L2** as the probe with a limit of detection based on 3σ of the blank of 3.4×10^{-7} M. Also, spectrofluorimetric titration curves of **L1**−**L3** with Hg^{2+} could only be fitted according to a 1:2 metal-to-ligand complexation model with association constants (log $K_{ass.}$) of 11.75(3), 11.96(1), and 11.24(1) calculated for the formation of the complexes $[Hg(\mathbf{L1})_2]^{2+}$, $[Hg(\mathbf{L2})_2]^{2+}$, and $[Hg(\mathbf{L3})_2]^{2+}$, respectively, in agreement with values calculated from spectrophotometric data (see above).[44] A partial CHEQ effect was observed for **L1**−**L3** in the presence of Ag^{+} (up to about 50%) and for **L1** and **L2** in the presence of K^{+} and Ca^{2+}, respectively. The other metal ions did not have an effect on the fluorescence emission intensity of **L1**−**L4** as significant as that observed for **L2** upon the addition of Hg^{2+}.

On the basis of the results discussed so far, the importance of the binding domain in the recognition process of anthracene-based fluorescent chemosensors exploiting the PET signaling principle and built according to a very flexible synthetic modular approach is clear. In general,

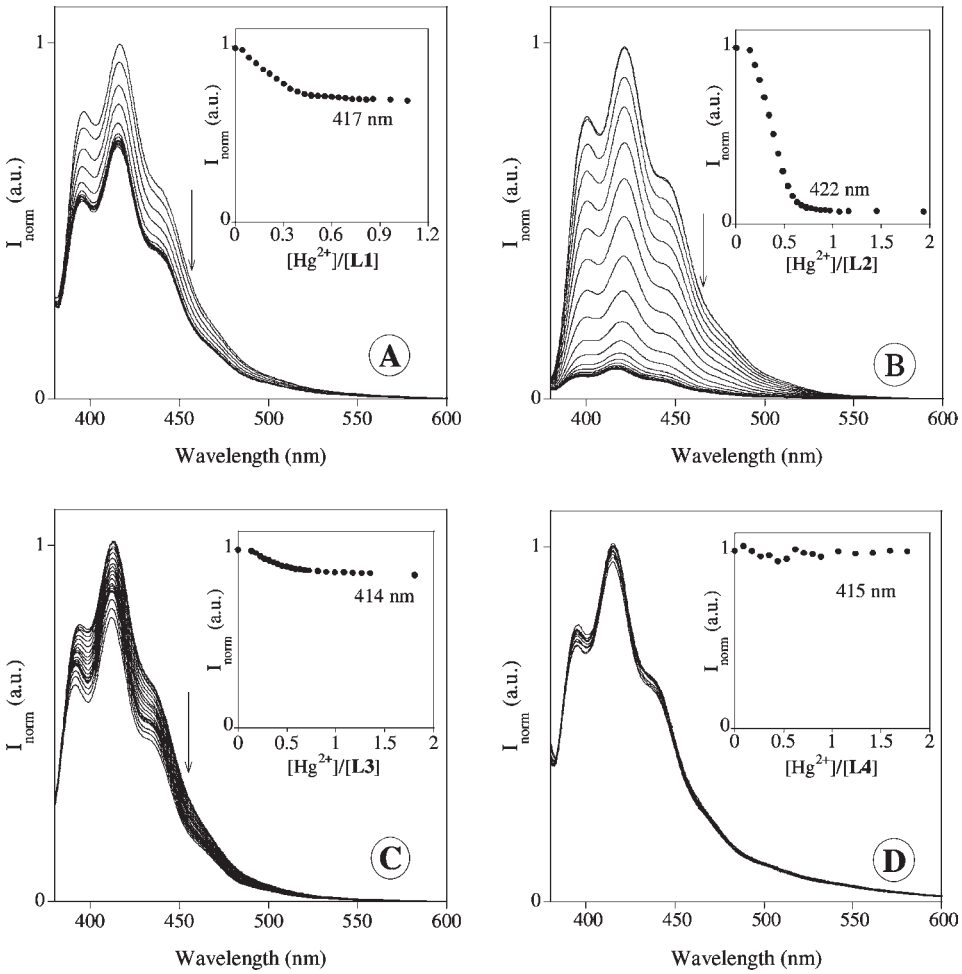

Figure 4. Normalized emission spectra of 1:1 (v/v) MeCN/H_2O solutions of **L1**−**L4** as a function of increasing amounts of added $Hg(CF_3SO_3)_2$. The insets show the normalized emission at the respective maximum wavelength. **L1** (A) (1.70×10^{-5} M; λ_{exc} = 367 nm; λ_{em} = 417 nm); **L2** (B) (1.50×10^{-5} M; λ_{exc} = 367 nm; λ_{em} = 422 nm); **L3** (C) (1.61×10^{-5} M; λ_{exc} = 367 nm; λ_{em} = 414 nm); **L4** (D) (0.82×10^{-5} M; λ_{exc} = 367 nm; λ_{em} = 415 nm).

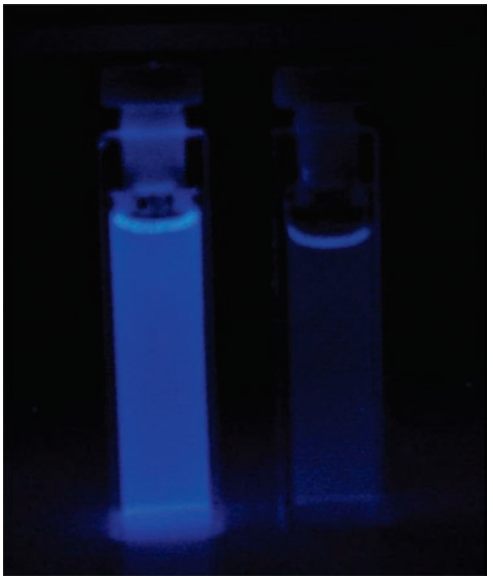

Figure 5. Photograph showing the color changes of **L2** before (left, 1.55×10^{-5} M) and after (right) the addition of 1 equiv of Hg^{2+} in a 1:1 (v/v) MeCN/H_2O solution upon UV irradiation.

as compared to analogous systems featuring azacrown ether and polyazacycloalkane receptor units,[12,39,45] the introduction of S-donor atoms in the cyclic framework moves, as expected, the selectivity of the supramolecular system, respectively, from alkali-metal and first-row transition-metal ions toward soft heavy-metal ions, in particular mercury(II). In the family of chemosensors here described, the NS_2O donor set of **L2** appears to be the best in guaranteeing a selective and stoichiometric "all" ON−OFF switchability of the signaling system in the presence of mercury(II), under the conditions considered. Interestingly, analogous selectivity toward mercury(II) in aqueous media has been observed in squaraine- and phenoxazinone-based integrated optical chemosensors featuring the same receptor unit as that in **L3**,[27b,c] whereas a fluorescein-based fluorescent chemosensor featuring 1-aza-4,7,10,13-tetrathiacyclopentadecane ([15]aneNS$_4$) has been reported to selectively detect mercury(II) in cells.[31] All of this clearly demonstrates the usefulness of sulfur-containing macrocycles in conjugation with fluorogenic units to achieve optical chemosensors for heavy-metal ions, in particular mercury(II);[26,30−32,42c] furthermore, the selectivity in the optical response depends on the supramolecular system

(45) (a) de Silva, A. P.; de Silva, S. A. *J. Chem. Soc., Chem. Commun.* **1986**, 1709. (b) Akkaya, E. U.; Huston, M. E.; Czarnik, A. W. *J. Am. Chem. Soc.* **1990**, *112*, 3590.

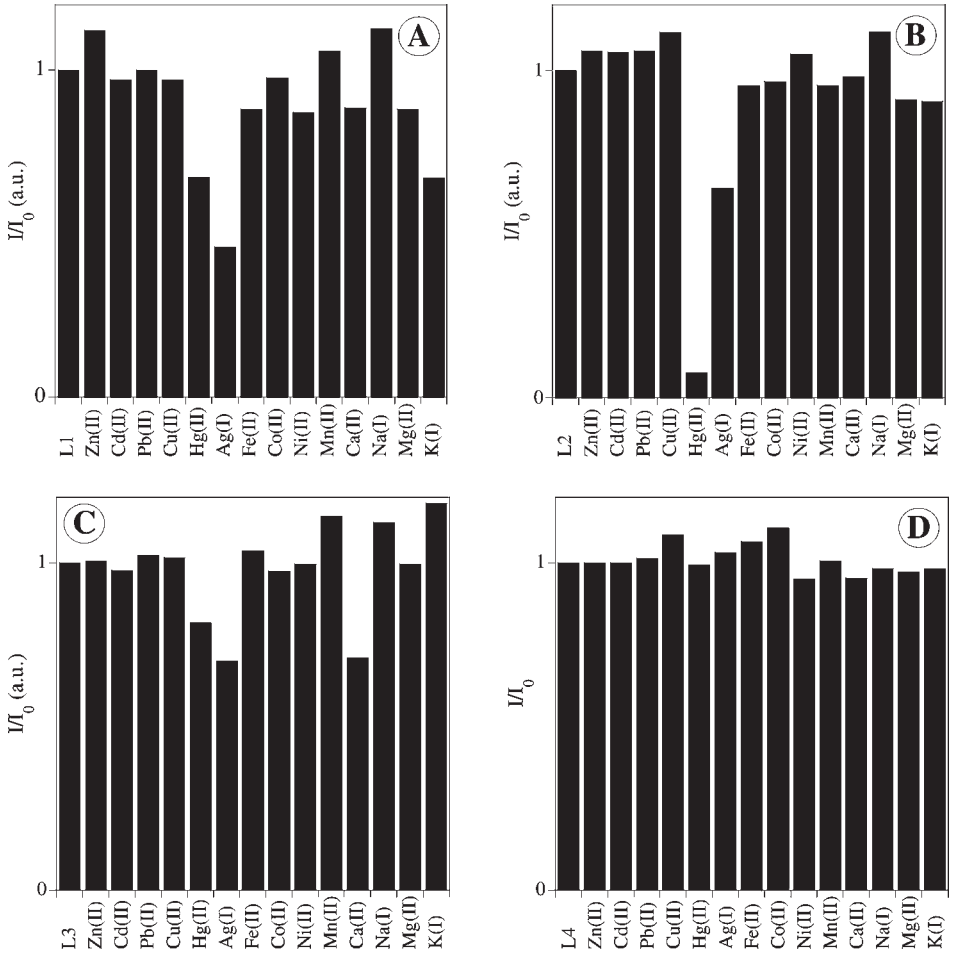

Figure 6. Relative emission intensity of **L1**−**L4** upon the addition of 10 equiv of Zn^{2+}, Cd^{2+}, Pb^{2+}, Cu^{2+}, Ag^{+}, Fe^{2+}, Co^{2+}, Ni^{2+}, Mn^{2+}, Ca^{2+}, Na^{+}, Mg^{2+}, or K^{+}: **L1** (A) (1.63×10^{-5} M; $\lambda_{exc} = 367$ nm; $\lambda_{em} = 417$ nm); **L2** (B) (1.42×10^{-5} M; $\lambda_{exc} = 367$ nm; $\lambda_{em} = 422$ nm); **L3** (C) (1.61×10^{-5} M; $\lambda_{exc} = 367$ nm; $\lambda_{em} = 414$ nm); **L4** (D) (0.82×10^{-5} M; $\lambda_{exc} = 367$ nm; $\lambda_{em} = 415$ nm).

as a whole and cannot be totally attributed to the characteristics of the bonding domain of the receptor unit, which, however, plays a crucial role, especially in PET-based emissive sensors. A vast compound library would be necessary for the rational design of PET sensors selective for each kind of metal ion target. Anthracene-based fluorescent chemosensors featuring sulfur-containing cyclic receptor units like **L1**−**L4** are, in general, also characterized by a high lipophilicity and could be used in the construction of chemical sensors like optomembranes, for the detection of heavy-metal ions in a sample of environmental and biological relevance, in real time and real space.

Following our investigation of the fundamental properties of **L1**−**L4**, all of the ligands were also explored using the NANODROP ND1000 spectrophotometer and ND3300 spectrofluorimeter. One or two drops (microliters) of the solution of each ligand in 1:1 (v/v) $MeCN/H_2O$ was placed on the optical pedestal, and the sample was drawn into a column and measured. The same experiment was repeated after the addition of 1 equiv of mercury(II). In Figure 7, the results obtained for all systems are reported, confirming the results obtained using classical spectrophotometers. The strongest quenching effect was observed after complexation of the ligand **L2** with Hg^{2+} (Figure 7B). The fine vibrational structure of the spectra was also maintained. This result is very interesting and confirms that small quantities of the ligand **L2** can be used for sensing purposes in confined spaces.

In order to have a full picture of the properties of all ligands as new emissive materials, the solid-state emission spectra of **L1**−**L4** were also recorded on a Horiba-Yvon-Spex Fluoromax-4 spectrofluorimeter using an external fiber-optic device. The normalized spectra are reported in the Supporting Information (Figure S2). Compared to the spectra recorded in solution (dotted lines), the spectra of **L1**−**L4** in the solid state show an unstructured red-shifted band at about 560 nm assigned to a preformed intermolecular excimer. This unstructured band is stronger in the case of the ligand **L4**, where two anthracene units are present in the chemical structure and an intramolecular excimer can also participate. This band is not observed in solution, presumably because of the low concentration used in our experiments.

As a part of our ongoing research project in exploring new fluorescence systems as MALDI-TOF-MS active probes, ligands **L1**−**L4** have also been studied in the gas phase.

Several MALDI-TOF-MS spectra were recorded using the free ligands dissolved in 1:1 (v/v) $MeCN/H_2O$ without any extra matrix and in the presence of 1 equiv of Ag^{+}, Cu^{2+}, and Hg^{2+}. The ligand peaks in the MALDI-TOF-MS positive mode appear at m/z 414.1 (**L1**), 398.20 (**L2**), 442.16 (**L3**), and 371.32 (**L4**); these peaks can be attributed

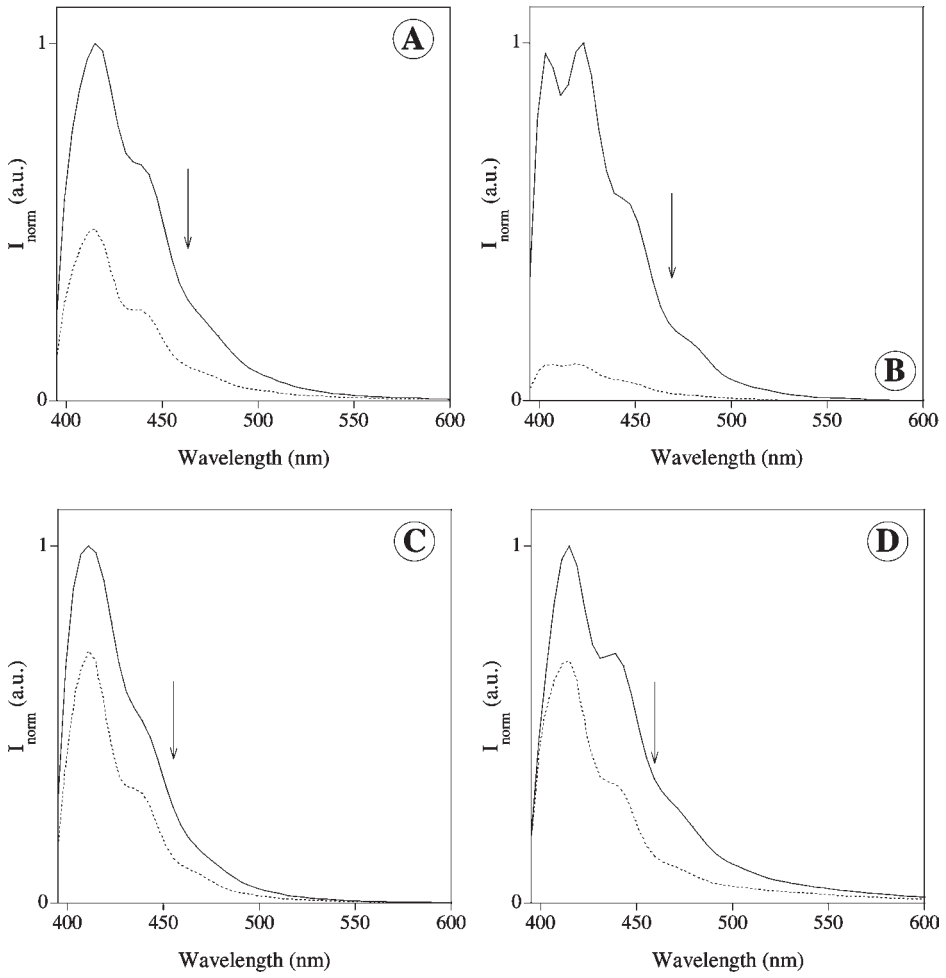

Figure 7. Normalized emission spectra of **L1**−**L4** registered by using NANODROP ND3300 technologies. The full lines represent the spectra of the free ligand. The dotted lines represent the spectra of the corresponding **L**/Hg^{2+} mixtures in a 1:1 molar ratio. **L1** (A) (1.63×10^{-5} M); **L2** (B) (1.42×10^{-5} M); **L3** (C) (1.61×10^{-4} M); **L4** (D) (1.35×10^{-4} M) in 1:1 (v/v) MeCN/H_2O at room temperature. The spectra were recorded during excitation of the samples using a UV LED (blue LED).

Table 1. Principal Peaks of MALDI-TOF MS Spectra of Free **L1**−**L4** Dissolved in 1:1 (v/v) MeCN/H_2O without Any Extra Matrix and in the Presence of 1 equiv of Ag^+, Cu^{2+}, and Hg^{2+}

	L1	L2	L3	L4
$[L + H]^+$	414.09 (26%)	398.20 (28%)	442.16 (35%)	371.32 (37%)
$[L + H]^{\bullet+}$	412.07 (100%)	396.21 (100%)	440.14 (100%)	569.32 (12%)
$[anthracene]^{\bullet+}$	191.05 (34%)	191.05 (44%)	191.05 (97%)	191.10 (100%)
$[L + Ag]^+$		505.99 (10%)	550.05 (29%)	
$[L + Ag]^{\bullet+}$	520.07 (21%)			677.11 (18%)
$[L + Cu]^+$	477.03 (42%)	461.13 (37%)	504.10 (21%)	
$[L + Cu]^{\bullet+}$				633.28 (5%)
$[L + Hg]^+$	613.8 (51%)	598.0 (82%)		

to the protonated species $[L + H]^+$. The peaks corresponding to the radical species $[L + H]^{\bullet+}$ and $[anthracene]^{\bullet+}$ were always present, and one or the other was the most intense peak (see Table 1).

In positive mode, upon the addition of 1 equiv of Ag^+, Cu^{2+}, or Hg^{2+}, the peak corresponding to the ligand was reduced in intensity, and a new peak(s) with 5−82% of intensity appeared (see Table 1), being more intense in the case of **L2** with Hg^{2+}; these peaks correspond to the mononuclear cationic species $[L + M]^+$ and/or to the radical species $[L + M]^{\bullet+}$ (Table 1). The pattern of the peaks observed in the MALDI-TOF-MS spectra fits well with the complex isotopic distribution simulated using the program from the DATA EXPLORER instrument. As can be seen in Table 1, ligands **L1** and **L2** react with all metals studied in the gas phase; however, in the spectra of ligands **L3** and **L4**, no peaks attributable to complex species with Hg^{2+} were observed.

DFT Calculations. Quantum-mechanical molecular-modeling techniques have been used to get structural and thermodynamic information on the complexes formed. Because of the good results obtained with ligand **L2** in solution as an ON−OFF fluorescent molecular sensor for Hg^{2+}, we have chosen to use this ligand as an example of the series and to optimize the structure of its 1:2 $[Hg(\mathbf{L2})_2]^{2+}$ complex.

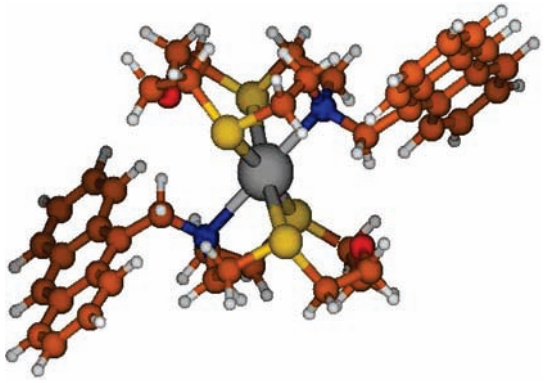

Figure 8. Most stable DFT-optimized structure for $[Hg(\mathbf{L2})_2]^{2+}$.

In order to tackle the complexity of the system, we used an "incremental approach". In the first place, we optimized the structure of the free macrocyclic unit [12]aneNS$_2$O, and subsequently the structure of its 1:1 complex with a naked mercury(II) cation (see Figure S3 in the Supporting Information). This structure would then serve as a scaffold to model the corresponding $[Hg\mathbf{L2}]^{2+}$ species and the sandwich-type complex $[Hg([12]aneNS_2O)_2]^{2+}$ (see Figures S4 and S5 in the Supporting Information). Once we obtained in this way the preferred binding patterns of the macrocyclic ligand [12]aneNS$_2$O to Hg^{2+} to form a 1:2 complex, we used these patterns to build different models for the complete system $[Hg(\mathbf{L2})_2]^{2+}$ (see Figure S6 in the Supporting Information).

The most stable optimized structures of the 1:2 complex cation $[Hg(\mathbf{L2})_2]^{2+}$ (see Figure 8) show the Hg^{2+} cation coordinated by the nitrogen and both S-donor atoms of each macrocyclic moiety in a distorted *pseudo*octahedral coordination geometry. The oxygen donors are not involved in metal coordination. This is in agreement with that observed in the X-ray crystal structure of the complex cation $[Hg([12]aneNS_2O)MeCN]^{2+}$, in which only a weak interaction is present between the metal center and the O-donor atom at 2.748(10) Å, while the other bond lengths at the metal center are significantly shorter [Hg−N 2.389(13) Å; Hg−S 2.550(3) and 2.521(4) Å].[17a]

The formation of the $[Hg(\mathbf{L2})_2]^{2+}$ sandwich-type complex is found to be favored by 26 kcal mol^{-1} (the gas-phase free energy) with respect to free **L2** and $[Hg\mathbf{L2}]^{2+}$.

The conformation of the macrocyclic moieties in the most stable optimized structure for the sandwich complex $[Hg(\mathbf{L2})_2]^{2+}$ leaves the anthracenyl groups on the coordination plane of the ligand and disposed of on opposite sides with respect to the metal center.

It is of note that the relative orientation of the two macrocycles in the three most stable optimized structures characterized by N−Hg−N angles of 180, 0, and 60° (N−Hg−N represents the angle between the nitrogen atoms of the ligands as projected on a plane containing the metal ion and perpendicular to the axis passing through the macrocyclic cavity center) has not large consequences on the stability of the corresponding 1:2 complexes in the gas phase (see the Supporting Information). Different orientations of the anthracene moieties are accompanied by a loss of coordination of the nitrogen atom(s) to the metal center and result in significantly higher energy values (see the Supporting Information). The disposition of the anthracene moieties in the three most stable optimized structures for $[Hg(\mathbf{L2})_2]^{2+}$ would permit intermolecular excimers.

Conclusions

A new family of emissive PET molecular probes, **L1**−**L4**, derived from [12]aneNS$_3$, [12]aneNS$_2$O, [15]aneNS$_2$O$_2$, and [12]aneN$_2$SO macrocyclic ligands containing NS$_3$, NS$_2$O, NS$_2$O$_2$, and N$_2$SO donor sets, respectively, and all featuring anthracene as the signaling unit, has been synthesized in good to excellent yields by a simple condensation reaction, and their photophysical properties have been evaluated in solution and in the solid state by absorption and fluorescence emission spectroscopy and by MALDI-TOF-MS in the gas phase.

Their capacity to act as a potential sensor for the metal ions Zn^{2+}, Cd^{2+}, Pb^{2+}, Cu^{2+}, Hg^{2+}, Ag^{+}, Fe^{2+}, Co^{2+}, Ni^{2+}, Mn^{2+}, Ca^{2+}, Na^{+}, Mg^{2+}, and K^{+} was carried out in 1:1 (v/v) MeCN/H$_2$O solutions. Among the cations studied, probe **L2** has shown a remarkable selectivity for Hg^{2+}, even when microsamples of **L2** were studied in the presence of mercury(II). This selectivity means that this new ligand could find application as a supramolecular chemosensor for this metal ion. DFT studies confirmed the formation of a sandwich-type 1:2 metal-to-ligand complex between **L2** and mercury(II) observed in solution as a favorable process.

Althougth fluorescent PET sensors based on anthracene are among the first fluorescent chemosensors to have been studied, understood, and developed, their natural ON−OFF ion-induced switchability, together with the simplicity of the synthetic routes by which such sensor molecules can be accessed, makes them still suitable for use in emerging fields of molecular switching devices. In particular, we believe that the use of sulfur-containing macrocycles as receptor units (nearly explored so far) may strongly contribute to the development of interesting new sensors for toxic heavy-metal ions, in particular mercury(II), based on the principle of PET.

Acknowledgment. We are indebted to InOU Uvigo through Project K914 122P 64702 (Spain) and FCT-Portugal through Project POCI/QUI/55519/2004 for financial support. J.L.C. and C.L. thank INCITE-Xunta de Galicia, Spain, for the Isidro Parga Pondal Research Program. V.L., C.C., and M.M. thank Ministero dell'Istruzione, dell'Università e della Ricerca, for financial support (Project PRIN 2007-C8RW53). We also thank Centro de Supercomputación de Galicia for the generous allocation of computational resources.

Supporting Information Available: Absorption and normalized emission spectra of **L1**−**L4** obtained after the addition of 1 equiv of NaOH (Figure S1), normalized solid-state emission spectra of **L1**−**L4** (Figure S2), DFT-optimized structures of the complexes $[Hg([12]aneNS_2O)]^{2+}$, $[Hg\mathbf{L2}]^{2+}$, $[Hg([12]aneNS_2O)_2]^{2+}$, and $[Hg(\mathbf{L2})_2]^{2+}$ (Figures S3−S6), relative free energies (kcal mol^{-1}) in the gas phase for all of the optimized structures of the complexes $[Hg([12]aneNS_2O)]^{2+}$, $[Hg\mathbf{L2}]^{2+}$, $[Hg([12]aneNS_2O)_2]^{2+}$, and $[Hg(\mathbf{L2})_2]^{2+}$ (Tables S2, S4, and S6), and geometric parameters for all of the optimized structures of the complexes $[Hg([12]aneNS_2O)]^{2+}$, $[Hg\mathbf{L2}]^{2+}$, $[Hg([12]aneNS_2O)_2]^{2+}$, and $[Hg(\mathbf{L2})_2]^{2+}$ (Tables S1, S3, and S5). This material is available free of charge via the Internet at http://pubs.acs.org.